Carbohydrate Research 344 (2009) 1701–1708

Contents lists available at ScienceDirect

Carbohydrate Research

journal homepage: www.elsevier.com/locate/carres

Fine structure characterization of amylopectins from grain amaranth starch

Xiangli Kong [a], Harold Corke [a], Eric Bertoft [b,*]

[a] School of Biological Sciences, The University of Hong Kong, Pokfulam Road, Hong Kong SAR, PR China
[b] Department of Food Science, Swedish University of Agricultural Sciences, PO Box 7051, S-750 07 Uppsala, Sweden

ARTICLE INFO

Article history:
Received 15 March 2009
Received in revised form 17 May 2009
Accepted 20 May 2009
Available online 17 June 2009

Keywords:
Amaranthus
Starch
Amylopectin
Cluster structure
Building blocks

ABSTRACT

The aim of this study was to determine the fine structure of amylopectin from grain amaranth. *Amaranthus* amylopectin was hydrolyzed with α-amylase, and single clusters and a group of clusters (domain) were isolated by methanol precipitation. The domain and the clusters were treated with phosphorylase *a* and then β-amylase to remove all external chains, whereby the internal structure was obtained. The ϕ,β-limit dextrins were analyzed on Sepharose CL 6B. The average DP (degree of polymerization) and peak-DP values of fractions of clusters were 57 and 82, respectively; the values of the domain were 137 and 309, respectively. The unit chain length profiles were analyzed by high-performance anion-exchange chromatography with pulsed amperometric detector (HPAEC–PAD). The results showed that the domain fraction contained ~2.2 clusters, and single clusters were composed of ~13 chains. The ϕ,β-limit dextrins of the clusters were further hydrolyzed with α-amylase to characterize their building block composition. The average DP of the branched blocks was ~11 and they contained on average ~2.5 chains. Their average chain length, internal chain length, and degree of branching were approximately 4.3, 2.8, and 14, respectively. A cluster consisted of ~6 branched blocks, and the internal chain length between the blocks was ~6.8.

1. Introduction

Starch is one of the most important biopolymers in nature, which provides the main dietary energy for human. Starch contains three types of biomacromolecules: amylopectin (which is highly branched), amylose (which is almost linear with few branches), and possibly an intermediate material, which is found in some kinds of starch (such as oat and some mutant maize genotypes[1,2]) and has a structure intermediate to those of amylose and amylopectin. There are large variations in the contents of the three components in starches from different sources, but amylopectin is commonly considered the major component in storage starch and accounts for about 65–85% by weight.[3] To describe the structural properties of amylopectin, the chain length profile is usually determined, but the cluster model of amylopectin, which can provide a useful conceptual basis for understanding of the structure of the biopolymer and guide current thinking related to amylopectin biosynthesis and physical behavior, has been given less attention.[4]

Grain amaranth is a pseudo-cereal with a long cultivation history in Central and South America, which produces very small seeds with high nutritional benefits. Starch is the main component in amaranth grain and has granules between 0.5 and 2.0 μm,[5–9] smaller than found in starches from most other sources. The starch granules possess A-type crystallinity, which is more compact than B-type crystallinity. Amylopectin is the major component in grain amaranth starch and has major effects on the properties. Little work has been done on the structure of amaranth amylopectin,[10–12] and this mainly focused on the molecular size of amylopectin. The internal and fine structure of amylopectin from amaranth is largely unknown. Recently, groups of clusters (structural domains) and clusters were isolated and characterized in potato amylopectin,[13,14] which provided a new approach to characterize the cluster structure of amylopectin. In these works, domains and clusters were isolated from amylopectin by an initial, short α-amylolysis, and a continued enzymatic hydrolysis, respectively; and building blocks were obtained by an extensive hydrolysis into near-limit dextrins with the liquefying α-amylase of *Bacillus subtilis*.[13,14] A cluster was defined as a group of chains in which the branches are found closer than ~9 residues from each other; domains are composed of more than one cluster interconnected by long chains (B2- and B3-chains); and building blocks were characterized as very densely branched areas in which the average internal chain length between branches was only ~2 glucosyl residues. Building blocks build up clusters by inter-block chains with an apparent length of 7–8 glucosyl residues.[13,14]

The objectives of this study were to: (i) produce and isolate a domain and clusters from amaranth amylopectins; (ii) characterize the structure of the isolated domain and clusters; (iii) characterize the building blocks in clusters.

* Corresponding author. Tel.: +46 18 672 048; fax: +46 18 672 995.
E-mail address: eric.bertoft@lmv.slu.se (E. Bertoft).

0008-6215/$ - see front matter © 2009 Elsevier Ltd. All rights reserved.
doi:10.1016/j.carres.2009.05.032

2. Experimental

2.1. Starch isolation, amylopectin fractionation, and debranching

Two amaranth cultivars, Cr049 and V69, were the same samples as in our previous report.[9] The starch isolation, amylopectin purification, ϕ,β-limit dextrin production from amylopectin, and debranching procedures were performed as previously described.[9,15]

2.2. Time course for α-amylolysis of amylopectins

Amylopectin (100 mg) was dissolved in 2 mL of 90% dimethyl sulfoxide (DMSO) with constant stirring for 2 days, then 7 mL hot MilliQ water was added. After cooling, 1 mL of 0.9 U/mL α-amylase of liquefying type (*B. subtilis*, also known as *Bacillus amyloliquefaciens*, EC 3.2.1.1, Seikagaku Corp., Tokyo, Japan) in 0.01 M sodium acetate buffer (pH 6.5) was added to start the reaction in a water bath (25 °C) with magnetic stirring. The enzyme activity was quantified on the day of analysis using Amylazyme assay (Megazyme, Wicklow, Ireland). Samples (100 μL) were taken every half hour from 0.5 h to 4 h. If analyzed immediately, 200 μL MilliQ water and 30 μL of 5 M NaOH were added and mixed; if not analyzed directly, 2 μL of 5 M NaOH was added and the sample was then stored at −20 °C. Prior to analysis, 200 μL MilliQ water and 30 μL of 5 M NaOH were added. The mixtures of the α-amylolysates were centrifuged and then analyzed by gel-permeation chromatography (GPC) on a column (1 × 90 cm) of Sepharose CL 6B (Pharmacia, Uppsala, Sweden) with 0.5 M NaOH as eluent at a rate of 0.5 mL/min.[13] The column was calibrated as described by Bertoft and Spoof.[16] The carbohydrate content of the collected fractions (0.5 mL) was determined by phenol–sulfuric acid reagent.[17]

2.3. Production of fractions of clusters and domains

The cluster and domain preparation was performed according to the method described by Bertoft[13] with some modifications and the procedure was similar to that described in Section 2.2. The amylopectin samples were incubated with α-amylase for the appropriate time (40 min for domain isolation and 3 h for cluster isolation) and the reaction was ended by adjusting the pH to ~13 with 5 M NaOH. After 1 h at room temperature, 5 volumes of methanol was added to the cluster preparations (1.2 volumes for domain preparations) and the solution was left at room temperature for another 1 h to precipitate the clusters or domains. The solution was centrifuged for 10 min at 1800*g*, the supernatant was removed, the precipitate was rinsed with methanol and centrifuged again. The precipitates were dissolved in 10 mL MilliQ water and were centrifuged to remove traces of undissolved matter, whereafter the supernatants were evaporated (Büchi Rotavapor R-3000, Flawil, Switzerland) at 60 °C to adjust the concentration to ~10 mg/mL. The concentrated samples were lyophilized (CT60e, Heto-Holten, Denmark) if not used directly for further experiments. An aliquot of 100 μL was taken for analyzing the molecular weight distribution on Sepharose CL 6B as described in Section 2.2.

2.4. Production of ϕ,β-limit dextrins

The production of ϕ,β-limit dextrins was conducted following Bertoft[13] with minor modifications. Samples of clusters or domain were dissolved in hot MilliQ water and adjusted to ~3 mg/mL. For 1 volume of the solution, 0.1 volume of 1.1 M sodium phosphate buffer (pH 6.8), 0.05 volumes of 2.8 mM EDTA, and 0.25 volumes of freshly prepared phosphorylase *a* solution (from rabbit muscle, ~25 U/mg, EC 2.4.1.1, Sigma–Aldrich, Deisenhofen, Germany; 2.5 mg dissolved in 25 mL MilliQ water) were added. The solution was stirred overnight at room temperature, the reaction was terminated in a boiling water bath for 5 min, the solution was centrifuged and the collected supernatant was reduced to 20% in volume by evaporation as in Section 2.3. The purification (removal of glucose 1-phosphate) was performed on two PD-10 columns (Sephadex G-25, Pharmacia, Uppsala, Sweden) coupled in series: 2 mL sample was applied on the columns followed by 3 mL MilliQ water. The eluate was discarded and then 4.5 mL MilliQ water was added and the sample was collected. The carbohydrate content was adjusted to ~3 mg/mL and the phosphorolysis and purification procedures were repeated to produce ϕ-limit dextrins. The carbohydrate concentration of purified ϕ-limit dextrin solution was adjusted to ~3 mg/mL, for 1 volume of the purified ϕ-limit dextrin solution, 1/3 volume 0.01 M sodium acetate buffer (pH 6.0) and β-amylase (from barley, 10,000 U/mL, EC 3.2.1.2, Megazyme, Wicklow, Ireland; ~4 U/mg substrate) were added, the solution was stirred overnight at room temperature and then placed in boiling water bath for 5 min to terminate the reaction. The solution was reduced to 20% of its original volume by rotary evaporation and was purified on PD-10 columns as described above. The β-amylolysis was repeated and the produced ϕ,β-limit dextrin was finally purified two times on PD-10 columns to completely remove maltose. The purified ϕ,β-limit dextrin was lyophilized or employed directly to perform the following analyses.

2.5. Analysis of fractions of ϕ,β-limit dextrins

The solutions of ϕ,β-limit dextrins were adjusted to ~3 mg/mL. (i) To 300 μL sample was added 30 μL of 5 M NaOH, the mixed sample was applied on Sepharose CL 6B as in Section 2.2. (ii) Unit chain length profile analyses of ϕ,β-limit dextrins were conducted as follows: 50 μL of 0.1 M sodium acetate buffer (pH 5.5) was added to 450 μL volume of the sample, 1 μL isoamylase (from *Pseudomonas amyloderamosa*, 250 U/mL, EC 3.2.1.68, Hayashibara Shoji Inc., Okayama, Japan) and 1 μL pullulanase (from *Klebsiella pneumoniae*, 429 U/mL, EC 3.2.1.41, Hayashibara Shoji Inc.) were added. The debranching reaction was conducted overnight at room temperature with slow constant stirring, the debranched samples were centrifuged and analyzed by HPAEC (Program 1 in Section 2.7).

2.6. Characterization of building blocks in ϕ,β-limit dextrins of clusters

ϕ,β-Limit dextrin (2 mg) was dissolved in 360 μL hot MilliQ water and 40 μL of 60 U/mL α-amylase in sodium acetate buffer (0.01 M, pH 6.5) was added. The α-amylolysis was conducted in water bath (35 °C) for 3 h and terminated in boiling water bath for 5 min. (i) 250 μL MilliQ water was added to 250 μL sample, then applied on a calibrated[16] column (1 × 90 cm) of Superdex 30 (Pharmacia, Uppsala, Sweden) with an elution rate of 0.5 mL/min (0.5 M NaCl). The carbohydrate content of collected fractions (0.5 mL) was analyzed by phenol–sulfuric acid reagent.[17] (ii) 470 μL MilliQ water was added to 30 μL sample, the solution was analyzed on HPAEC (Program 2 in Section 2.7). (iii) To another 30 μL sample were added 470 μL MilliQ water, 50 μL of 0.01 M sodium acetate (pH 5.5), 1 μL isoamylase, and 1 μL pullulanase, the debranching reaction was performed overnight as in Section 2.5. The debranched sample was boiled to terminate the reaction and was then analyzed by HPAEC (Program 2 in Section 2.7).

2.7. High-performance anion-exchange chromatography (HPAEC)

The high-performance anion-exchange chromatography (Series 4500i, Dionex Corp., Sunnyvale, CA, USA) equipped with a BioLC

gradient pump and a pulsed amperometric detector (PAD) was employed in this study, with two different gradient programs. Program 1 was the same as in our previous report.[15] Program 2 was conducted according to the method in Bertoft[14] with some modifications: The column (250 × 4 mm, Carbo-Pac PA-100 with guard column) was eluted with a mixture of 150 mM NaOH (eluent A) and 150 mM NaOH containing 1 M NaOAc (eluent B) at the rate of 1 mL/min. The elution gradient was as follows: from 0 to 1.3 min, 93% eluent A; from 1.3 to 16 min, eluent A changed from 93% to 83% linearly; 16–27 min, from 83% to 80%; 27–53 min, from 80% to 76%; 53–55 min, from 76% to 50%; 55–59 min, 50%; 59–61 min, from 50% to 93% (return to start mixture). The sample was injected during the initial 1.2–1.3 min. The PAD signal was recorded by POWERCHROM software program (eDAQ Pty Ltd, Australia) and corrected to carbohydrate content according to Koch et al.[18]

3. Results

3.1. α-Amylolysis of amylopectins fractionated from grain amaranth starch

The molecular weight distribution of the α-amylolysates of amylopectins from one of the amaranth cultivars, Cr049, is shown in Figure 1. The trend of sample V69 was very similar to Cr049. The α-amylolysis of amylopectin was characterized as a non-random process, which was generally in agreement with the previous reports in potato amylopectin,[19] waxy rice starch,[20] and maize mutant starches.[21] After 1 h of enzymatic hydrolysis, a typically bimodal distribution representing fractions of domains or clusters (fraction A in Fig. 1a) and small fragments mostly derived from the external chains (fraction B), respectively, was observed. The molecular weight range of the samples became narrower with hydrolysis time, and after 3 h the changes were very small. The DP of the peaks ranged between ~80 and ~160 at the later stages, which was consistent with a previous report for waxy-rice starch.[20] The average DP of the larger molecular mass fraction (fraction A) versus hydrolysis time is also presented (Fig. 1b). Initially, DP decreased very fast but after ~3 h the changes with time were small possibly because the long chain segments between the clusters that are easily attacked[22] had been cleaved at earlier stages, suggesting that the reaction mixture mainly contained clusters of chains that were comparatively resistant to the enzymatic attack.

Based on the above-mentioned results, 40 min and 3 h were chosen as enzymatic hydrolysis time for the production of a domain fraction from sample Cr049 (designated Cr049-I) and cluster fractions from both amaranth samples (Cr049-II and V69-II). The branched dextrins (represented by fraction A in Fig. 1a) were collected by precipitation in methanol–water solutions.

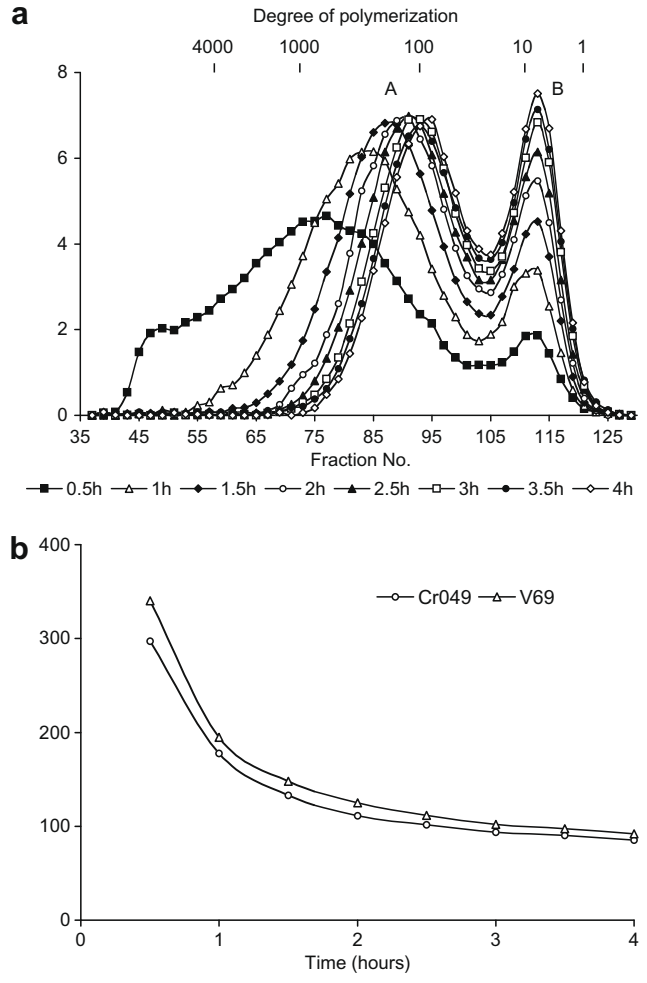

Figure 1. Time course for α-amylolysis of amaranth amylopectins. (a) Gel-permeation chromatography on Sepharose CL 6B of cultivar Cr049. Two major fractions of dextrins with DP >30 (fraction A) and <30 (B) were formed. (b) The decrease in DP of fraction A.

3.2. Characterization of ϕ,β-limit dextrins

ϕ,β-Limit dextrins were obtained by removing external chain stubs, which remained after α-amylolysis, with successive treatments with phosphorylase *a*- and β-amylase. After removing the external chains, it was possible to compare the remaining inner structure of the domain and clusters.[13,23] The average DP and peak-DP values of the ϕ,β-limit dextrins of the fractions of clusters (57 and 82, respectively) were similar in the two different amaranth amylopectin samples (Fig. 2 and Table 1). Corresponding values of the domain fraction of sample Cr049 were 137 and 309, respectively.

The samples of limit dextrins were debranched and the internal unit chain distributions were analyzed by HPAEC–PAD (Fig. 3). The average chain lengths (CLs) of the ϕ,β-limit dextrins from fractions of clusters were 6.2–6.4, which were shorter than those of the amylopectins (7.7–7.8) and the domain (8.1) because the longer chains between clusters had been cleaved by the α-amylase. The average internal chain length (ICL) of the ϕ,β-limit dextrins possessed a similar trend and the total internal chain length (TICL) decreased with increasing time of α-amylolysis. The average number

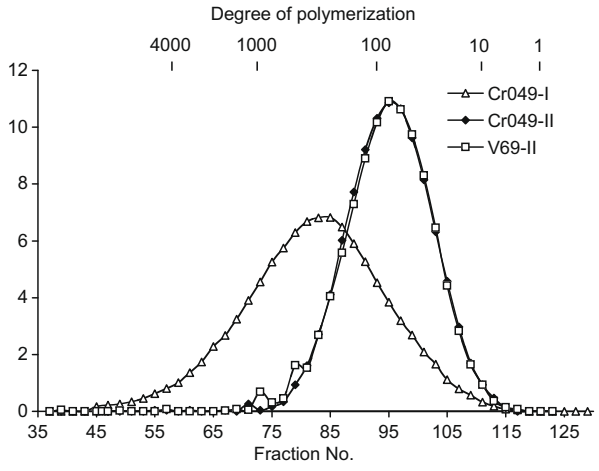

Figure 2. Molecular weight distributions on Sepharose CL 6B of ϕ,β-limit dextrins of fractions of clusters and a domain from amaranth amylopectins.

Table 1
Characterization of ϕ,β-limit dextrins of amylopectins (APs), domains (I), and clusters (II) prepared from starches of the amaranth varieties Cr049 and V69

Samples	DP[a]	Peak-DP[a]	CL[b]	ICL[c]	TICL[d]	NC[e]	Peak-NC[f]	DB[g]
Cr049-AP	—	—	7.7	5.2	13.5	—	—	—
V69-AP	—	—	7.8	5.3	13.3	—	—	—
Cr049-I	137	309	8.1	5.9	11.8	16.9	38.2	11.6
Cr049-II	57	82	6.4	4.5	10.3	8.8	12.8	13.8
V69-II	57	82	6.2	4.3	10.5	9.1	13.3	14.4

[a] DP and peak-DP values from GPC on Sepharose CL 6B.
[b] Average chain length obtained by HPAEC–PAD of debranched samples.
[c] Average internal chain length = CL − ECL − 1, in which ECL is 1.5 in ϕ,β-limit dextrins, or when NC is known ICL = [(CL − ECL) × NC/(NC − 1)] − 1.
[d] Total internal chain length of B-chains obtained by HPAEC–PAD.
[e] Number of chains = DP/CL.
[f] Number of chains at peak-DP = peak-DP/CL.
[g] Density of branches (as percent) = (NC − 1)/DP × 100, in which (NC − 1) equals the number of branches.

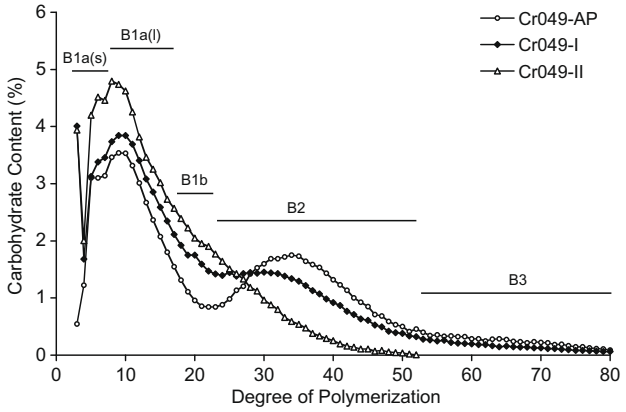

Figure 3. Chain length profile obtained by HPAEC of the ϕ,β-limit dextrins of amylopectin, a domain, and clusters of amaranth starch sample Cr049 (only B-chains are shown).

of chains (NCs) and number of chains at peak-DP (peak-NCs) decreased significantly from domain to clusters. The degree of branching (or density of branches, DB) increased from 11.6% to ~14% (Table 1).

3.3. Unit chain composition of clusters

The unit chains in amylopectin are divided into A-chains (unsubstituted) and short (BS) and long B-chains (BL).[24] Bertoft[13] sub-categorized the B-chains in limit dextrins as shown in Figure 3 into very short B1a(s)-chains (or 'fingerprint' chains), longer B1a(l)-chains, B1b-chains, B2-chains, and B3-chains, respectively. In the ϕ,β-limit dextrins, A-chains appear as maltosyl residues[25] (they are not shown in Fig. 3). However, some A-chains are also

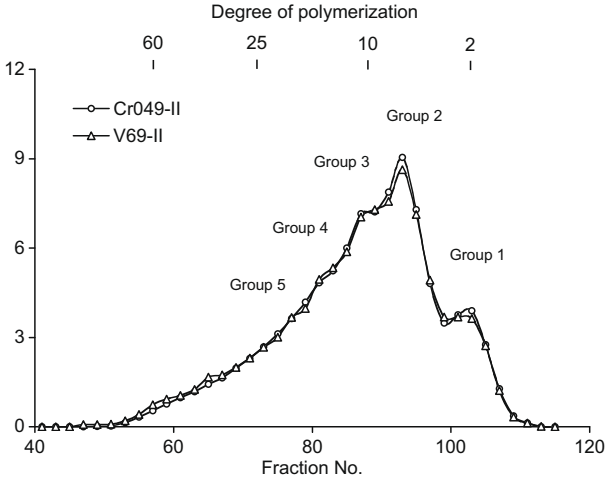

Figure 4. Size distribution on Superdex 30 of near-limit dextrins from clusters obtained by extensive treatment with α-amylase for 3 h. Groups of building blocks are indicated.

found as maltotriosyl residues due to their previous size reduction by the α-amylase.[13] This fraction of A-chains was detected in the debranched samples of the α-dextrins (not shown) and was corrected for in the calculations of the molar amounts of the different chain categories, which are presented in Table 2. The relative amounts of A- and BL-chains were lower in the isolated clusters than in the amylopectins. Apparently, BL-chains were cleaved into BS-chains during cluster isolation, thereby increasing the molar amounts of mostly B1b- and B1a(s)-chains at DP 18–22 and 3–7, respectively. Of the latter chains, the increase was mostly due to a production of chains of DP 3, that is, the shortest possible type of B-chain.

3.4. Characterization of building blocks in clusters

The ϕ,β-limit dextrins of clusters were further extensively hydrolyzed by a concentrated solution of α-amylase (6 U/mL) for 3 h to characterize the profile of the building block composition in the clusters. The molecular weight distribution of produced dextrins, which were almost resistant to further enzymatic hydrolysis[20] and characterized as near-limit dextrins,[14] was analyzed by gel-permeation chromatography on Superdex 30, the result is shown in Figure 4. The clusters from the two amylopectin samples showed identical compositions of near-limit dextrins, a major group of the dextrins showed a peak at DP 7. The near-limit dextrins can be divided into linear dextrins (group 1 with peak at DP ~2) and tightly branched dextrins (the latter were called building blocks). From previous characterization of the building blocks in potato amylopectin,[14] it is known that building blocks of groups 2, 3, and 4 contain 2, 3, and approx. 4 chains, respectively, whereas group 5 consists of multiply branched blocks.

Table 2
Molar amounts (as percent) of chain categories in two varieties (Cr049 and V69) of amaranth amylopectins (APs) and their clusters (II)[a]

	A	DP 3	B1a(s)	B1a(l)	B1b	B2	B3	BS	BL
Cr049-AP	54.45	1.40	15.97	18.85	1.99	7.83	0.90	36.82	8.73
V69-AP	52.47	2.21	17.45	19.29	1.96	7.83	1.00	38.71	8.83
Cr049-II	50.07	11.54	22.42	19.57	4.23	3.71	-	46.22	3.71
V69-II	49.16	11.98	21.92	21.50	4.09	3.84	-	47.50	3.84

[a] A-chains were estimated as the amount of maltose obtained after debranching (for amylopectins) and correction with A-chains in the form of maltotriose (for α-dextrins)[13]; BS are short chains of DP 3–22, of which B1a(s) are very short at DP 3–7, DP 3 is the shortest type of B1a(s), B1a(l) have DP 8–17, and B1b have DP 18–22; BL are long chains with DP ⩾ 23, of which B2-chains possess DP 23–52 and B3-chains DP ⩾ 53.

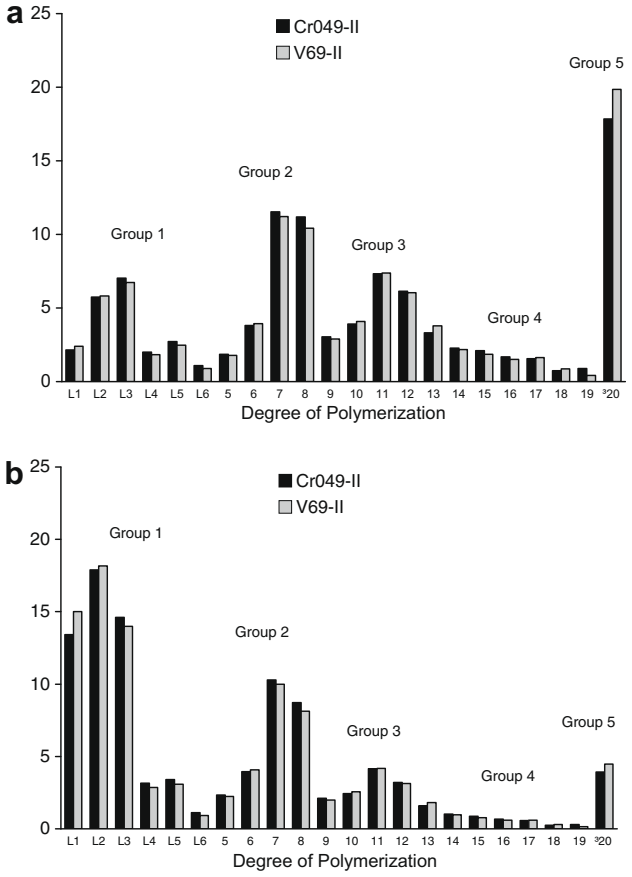

Figure 5. Bar graph representation of the size distribution of building blocks in clusters obtained by HPAEC (L in front of the chain number means linear dextrins). (a) Weight-based and (b) molar-based. Groups of building blocks are indicated.

The produced near-limit dextrins were also analyzed before and after debranching by HPAEC, by which a good resolution of the dextrins is obtained at DP <20.[14] The size distribution of linear dextrins and branched building blocks is presented in Figure 5. Branched blocks can be distinguished from linear blocks because the former are eluted from the anion-exchange column before the linear blocks with a similar DP.[26] The carbohydrate content at DP >19 from HPAEC (collected in a single peak by a sharp increase of the sodium acetate gradient) agreed well with that from GPC. From the production of linear dextrins after debranching it was possible to estimate the composition of chains in the branched blocks.[14] The general structure characterization of building blocks of clusters is summarized in Table 3. The average DP of the α-amylolysates of the clusters was ~6.3. The molar percentage of linear building blocks was ~54%, but on a weight basis the branched blocks predominated. Their average DP was ~11. After the blocks were debranched, their structural parameters could be calculated. The values of CL, ICL, NC, and DB of branched building blocks from the two amaranth samples were very similar, approximately 4.3, 2.8, 2.5, and 14, respectively.

Table 3
Characterization of the structure of building blocks in fractions containing clusters

Samples	Whole DP[a]	Linear[b]		Branched[c]						
		Mol (%)	DP	Weight (%)	Mol (%)	DP-Blocks	CL[d]	ICL[e]	NC[f]	DB[g]
Cr049-II	6.3	53.6	2.4	79.3	46.4	10.7	4.3	2.8	2.5	14.1
V69-II	6.3	54.2	2.3	79.9	45.8	10.9	4.4	2.9	2.5	13.8

[a] Average values of the whole sample.
[b] Linear dextrins of DP 1–6.
[c] Branched building blocks of DP ⩾ 5.
[d] Chain length obtained by debranching and subtraction of linear dextrins.
[e] Average internal chain length = (CL − ECL) × NC/(NC − 1) − 1, in which ECL is estimated to be 2 in the building blocks.
[f] Number of chains = DP/CL.
[g] Density of branches = (NC − 1)/DP × 100.

Table 4
Compositions of building blocks in clusters

Samples	No. of blocks[a]	Density of blocks[b]	Molar distribution of groups of blocks[c] (%)			
			2	3	4	5
Cr049-II	4.2	7.4	54.5	29.1	7.9	8.4
V69-II	4.1	7.3	53.2	29.8	7.3	9.8

[a] Estimated number of blocks at average DP (Table 1).
[b] (Number of blocks)/(DP of fraction) × 100.
[c] Group 2 (DP 5–8), 3 (9–13), 4 (14–19), and 5 (⩾20).

From the weight-based distribution, it is possible to calculate the molar distribution of different blocks (Fig. 5b). Group 2 (DP 5–8), which contained only 2 chains, predominated in the clusters (Table 4). Altogether a typical cluster (with a size corresponding to the average DP) was build up from ~4 blocks and the density of the blocks in the clusters was 7.3–7.4.

4. Discussion

The molecular structure of amylopectin can be described through the three structural levels of domains, clusters, and building blocks. Clusters of branches constitute the basis in the cluster model and are generally believed to consist of the short unit chains of DP 6–35.[24] Clusters are interconnected through the long BL-chains into smaller or larger groups that were called structural domains.[20] Inside the clusters the chains are organized into smaller, very tightly branched groups of building blocks.[14,20] In this work on the amylopectin component in amaranth starches we investigated all three structural levels.

4.1. Constitution of clusters in amaranth amylopectin

When employing the liquefying α-amylase of *B. subtilis* to hydrolyze the amylopectin, the BL-chains are easily attacked, while short chains are relatively resistant to hydrolysis.[27] In this way clusters can be released from the amylopectin (Fig. 1). The clusters isolated in the current study were apparently of rather homogenous sizes with an average DP of 57 in both amaranth samples (Table 1). The peak-DP position of the isolated cluster fraction in gel-permeation chromatograms was 82. The clusters were similar in size to those of the double mutant *wxdu* maize,[21] which, like amaranth starch granules, was defined as having A-type crystallinity. In contrast, the amylopectins of potato and *aewx* maize,[13,21] which are B-crystalline starches, possessed somewhat smaller clusters. The fine structures of the clusters were apparently specific to the different plant species as shown by the variations of the structural parameters (Table 1), such as the average CL of the clusters, which in amaranth was shorter than that reported previously for potato,[13] but longer than that reported for *wxdu* maize starch.[21] This was also reflected in the degree of branching (DB) in the domain and clusters (Table 1), which was similar to the results observed in waxy rice,[28] but larger than those observed in potato amylopectin starch[13] and *aewx* maize starches.[21] This suggests that clusters in A-crystalline starches are more densely branched than in B-types.

4.2. Mode of cluster interconnection

The constitutions of unit chains in the isolated clusters were different from the original amylopectin samples (Table 2). The relative molar amount of A-chains decreased after the action of the α-amylase and in isolated clusters the ratio of A:B-chains was close to 1, which suggested that each double helix of the cluster was formed by one A- and one B-chain in accordance with molecular modeling of this structure using data obtained from crystallographic studies of small oligosaccharides.[29,30] As the ratio decreased, there was a simultaneous increase in the amount of B-chains. Most probably, therefore, the cleavage of the long B2- and B3-chains (Fig. 3) spanning between the clusters preferentially resulted in the formation of new B-chains (rather than one B- plus one A-chain). In Figure 6, the changes in chain composition as a result of the amylase attack are illustrated on a molar basis and it is seen that the attack gave rise preferentially to certain types of the sub-categories of the B-chains. Thus, chains of intermediate lengths between long and short chains were formed in the range corresponding to shorter B2-chains (at DP 23–27) and longer B1-chains, here designated B1b-chains (DP 18–22). Similar results were obtained previously with the amylopectins from rice, maize, and potato, which suggests a common mode of cluster interconnection in these samples.

Besides the formation of the chains of intermediate length, chains corresponding to the short chains of group B1a(s) were also formed (Fig. 6). On a molar basis, B1a(s) constituted 16–17% of the chains in the amylopectin samples and ~22% in the isolated clusters (Table 2), that is, an increase of ~6%. This corresponded roughly to the apparent amount of formed B1b- and B2-chains in the clusters (7.9% of B1b + B2 subtracted with 2% pre-existing B1b-chains in the amylopectins). As illustrated in Figure 7, it appears therefore that the long B2- and B3-chains were cleaved preferentially at internal chain segments between the clusters into two new B-chains, of which one had a length of DP 18–27 (B1b- and shorter B2-chains) and the other had a very short internal chain corresponding to B1a(s). After the cleavage by the α-amylase, the latter chain might carry an external chain segment, which however, was removed when the clusters were transformed into the ϕ,β-LD:s. It is interesting to notice that the shortest possible type of B-chain with DP 3, which originally was a minor type in amylopectin, increased most significantly of all single types of chain lengths when the domain and clusters were isolated, so that it represented not less than one half of all the B1a(s)-chains. This strongly suggested a special mode of starch synthesis leading to a preferential type of interconnection of the clusters in amaranth amylopectin. As schematically illustrated in Figure 7, the interconnecting B-chain typically carries a chain (which might be either an A- or B-chain) very close to its reducing-end side and connects to the other cluster through an extended internal segment, apparently free from other branches. A similar type of cluster interconnection appeared to be common in waxy rice amylopectin, but in potato only in some structural domains.

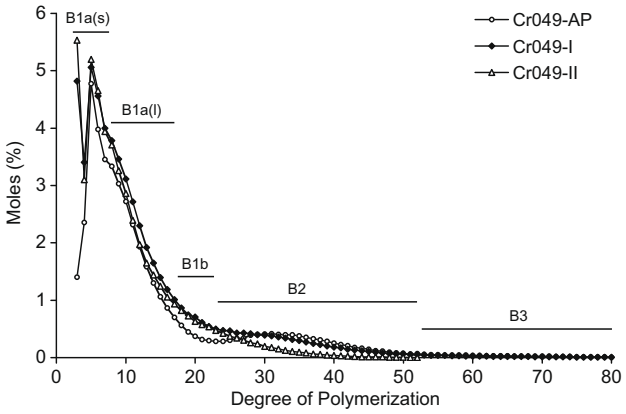

Figure 6. Molar-based internal unit chain profiles of amylopectin and a domain and clusters isolated from amaranth starch.

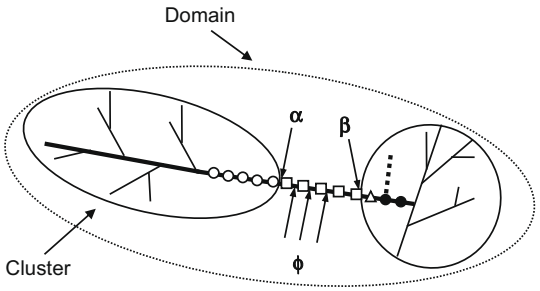

Figure 7. Possible preferential mode of cluster interconnection in amaranth amylopectin. Two clusters in a hypothetical limit dextrin of a domain are interconnected through a long B-chain (bold line). Glucosyl residues involved in the inter-cluster chain length (IC-CL) are shown as white symbols. Squares show residues forming the inter-cluster degree of polymerization (IC-DP), which constitute the external chain of the cluster to the right after the attack by α-amylase (α). This chain is removed by the successive treatments with phosphorylase (ϕ) and β-amylase (β). The residual chain on the right-hand cluster contains a single external residue (triangle) and two internal residues (black circles) and is detected as the shortest possible B-chain of DP 3 in the subsequent analyses. The dotted line represents a chain (A- or B-chain) on the closest possible position next to the (1→6)-linkage of the inter-cluster chain. The residual chain on the left-hand cluster corresponds to B1b- or short B2-chains with DP 18–27 with an internal chain stub at the reducing end with ~5 residues (white circles).

It is possible to estimate the average size of the chain segment separating two clusters (inter-cluster DP, IC-DP) in the domain fraction of the amylopectin (Fig. 7) when the number of clusters in the domain is known.[13] As one chain of each cluster extends into another cluster, the number of clusters approximately equals the number of chains in the domain (NC_{domain}) divided by $NC_{cluster} - 1$. The average number of clusters in the domain was 2.2 (Table 5). IC-DP is then estimated as the difference between the total DP that the clusters of the domain occupy and the DP of the domain (i.e., IC-DP = ($DP_{domain} - DP_{cluster} \times$ No. of clusters)/No. of clusters). IC-DP was 5.3 residues (Table 5) and this thus represented the part of the inter-cluster segment that was removed by the action of both the α-amylase and the successive actions of the phosphorylase and β-amylase. However, as the enzymes are not attacking the linkages close to the branches, the actual chain length of the inter-cluster segment (IC-CL) was longer (Fig. 7). A theoretical value of IC-CL in a domain can be estimated if it is assumed that there are

Table 5
Characterization of the cluster structure of amaranth amylopectins (APs) and a domain fraction (I)

Samples[a]	No. of clusters[b]	IC-DP[c]	IC-CL[d]
Cr049-AP	—	—	10.7
V69-AP	—	—	13.4
Cr049-I	2.2	5.3	13.8

[a] Amylopectin (AP) and a domain sample (I) from cultivars Cr049 and V69.

[b] Number of clusters = $NC_{domain}/(NC_{cluster} - 1)$, in which NC is the number of chains.

[c] Average inter-cluster degree of polymerization = ($DP_{domain} - DP_{cluster} \times$ No. of clusters)/No. of clusters.

[d] Inter-cluster chain length was estimated in amylopectins as $IC\text{-}CL_{ap} = [ICL_{ap} \times (NIC_{cluster} + 1)] - (ICL_{cluster} \times NIC_{cluster})$, and in domain as $IC\text{-}CL_{domain} = [(ICL_{domain} \times NIC_{domain}) - (ICL_{cluster} \times NIC_{cluster} \times$ No. of clusters)]/(No. of clusters − 1), in which (No. of clusters − 1) equals the number of inter-cluster segments. NIC is the number of internal chains (which equals NC − 1).

no branches appearing outside the clusters in the inter-cluster segment by comparing the total number of glucosyl residues included in the internal chains of the domain with those in the clusters:

$$\text{IC-CL}_{\text{domain}} = [(\text{ICL}_{\text{domain}} \times \text{NIC}_{\text{domain}}) - (\text{ICL}_{\text{cluster}} \times \text{NIC}_{\text{cluster}} \times \text{No. of clusters})]/(\text{No. of clusters} - 1),$$

in which NIC is the number of internal chains (NIC = NC − 1). As ICL of the original amylopectin molecule includes all internal chains (within as well as between clusters), it is also possible to estimate an average value for the whole amylopectin (IC-CL_{ap}, Fig. 7) as

$$\text{IC-CL}_{\text{ap}} = [\text{ICL}_{\text{ap}} \times (\text{NIC}_{\text{cluster}} + 1)] - (\text{ICL}_{\text{cluster}} \times \text{NIC}_{\text{cluster}})$$

In the domain isolated from sample Cr049, the IC-CL_{domain} was 13.8, which agreed fairly well with IC-CL_{ap} of Cr049 and V69 (10.7 and 13.4, respectively, Table 5). The difference between IC-CL and IC-DP (5.4–8.5 residues) reflected the length of the internal chain at the reducing end of one of the clusters which was left after α-amylase attack (Fig. 7).

4.3. Internal structure of the clusters

Turning from the inter-cluster to the intra-cluster structure, the molar composition of chains given in Table 2 was used to calculate the constitution of unit chains of the isolated clusters. At peak-DP, which represented the major part of isolated clusters on a weight basis, the NC of the clusters was 12.8–13.3 (Table 1). The number was similar to that found for clusters from *wxdu* maize[21] and larger than previously reported in the B-crystalline samples of potato and *aewx* maize.[13,21]

The number of chains of each category in the clusters is exhibited in Table 6. No difference was observed in the composition of chains in the clusters between the two different amaranth amylopectins. In the isolated clusters, the sum of B1b- and B2-chains was 1.0, which strongly suggested that they indeed represented a single type of chain that was formed when the α-amylase hydrolyzed the long chains between the clusters and represented the basis of the cluster onto which the rest of the chains were attached. Each cluster contained ~1.5 chains of the shortest type at DP 3. As discussed above, one such chain was probably formed as a result of the cleavage of the inter-cluster chain, whereas the rest (0.5 chains) suggested that some clusters also possessed these chains already in the original amylopectin molecule. The rest of the clusters was formed by 1–2 chains of the other B1a(s) (DP 4-7), 2–3 B1a(l), and 6–7 A-chains.

The chains of the clusters were arranged in a specific way that allowed the α-amylase to attack somewhat longer chain segments between branches, leading to the release of the building blocks. The size distribution of the blocks (Figs. 4 and 5) resembled that found in potato clusters,[14] but was different from those observed in waxy-rice and *wxdu* maize.[20,21] From the molar distribution of the blocks (Table 4), it was possible to estimate the building block structure of a cluster of DP 82 (peak-DP). At this DP, the chains of the cluster formed ~6 branched blocks, of which about half possessed DP 5–8 (group 2) and contained only a single branch point (Table 7). Approximately two of the blocks had two branches (group 3), whereas a block with either three or multiple branches (groups 4 and 5, respectively) apparently was distributed evenly in every second cluster.

It was also possible to estimate the inter-block DP (IB-DP) inside the clusters (Table 7) from the formation of the linear blocks at DP 1–6, which come from α-amylase attack on the internal chains that connect the branched blocks.[14] IB-DP was about 2.8 residues and was shorter than observed in potato amylopectin (3.1–4.5).[14] The actual average ICL between the branches of two adjacent building blocks (inter-block CL, IB-CL) is longer, however, because the enzyme cannot attack the glucosidic linkages next to the branches.[31] Therefore, IB-CL approximately equals[14] IB-DP + 4 and was ~6.8. As expected from the suggested structural definition of a cluster,[14] the length between the building blocks inside the clusters was thus <9 residues and much shorter than the inter-cluster chain length (IC-CL, 10.7–13.8, Table 5).

Though the size distribution of the building blocks of amaranth amylopectin possessed clear similarities to clusters of potato amylopectin, suggesting a similar organization of the blocks inside the clusters,[14] it is important to notice that several structural parameters (besides the larger size of the clusters in amaranth) were different. As noted above, IB-DP (and IB-CL) was shorter in amaranth amylopectin, showing that the blocks were more densely packed in the clusters. The structural parameters of the building blocks were also different. Thus, their average ICL was longer (2.8–2.9, Table 3) and therefore they were less densely branched than in potato (in which the ICL inside the blocks was 1.7–2.2).[14] Molecular modeling was performed theoretically on small building blocks consisting of two interlinked double helices, that is, blocks consisting of three branches.[32] It was found that only certain combinations of ICL-values gave rise to parallel conformations of the two adjacent double helices. Thus, ICL-values of 1 + 3 (average ICL 2) corresponded to the A-allomorph, whereas 4 + 6 (average 5) might be either A- or B-allomorph. These values did not find experimental support in amaranth (A-) and potato (B-allomorph). However, ICL values of 7 + 7 also resulted in parallel double helices[32] and match therefore closely the experimentally found value for IB-CL in amaranth (Table 7). Indeed, a recent work on the molecular composition of the crystalline lamellae in waxy-maize starch, isolated as distinct nano-crystals, suggested that the lamellae constitute a complex co-operative structure, in which non-adjacent double helices from a large number of building blocks and clusters participate.[33]

It was also interesting to find that there existed differences in the internal unit chain distribution of the amylopectin macromolecules from amaranth and potato. The distribution of amaranth amylopectin chains (Fig. 3) resembled that of rice and maize, which were recently distinguished as belonging to 'type 2' internal structure, whereas potato belongs to 'type 4', which typically possesses less B1a(s)-chains and more B3-chains.[23] Such differences

Table 6
Composition of chains in clusters in ϕ,β-limit dextrin at peak-DP[a]

Samples	Chain category[b]					
	A	DP3	B1a(s)	B1a(l)	B1b	B2
Cr049-II	6.4	1.5	2.9	2.5	0.5	0.5
V69-II	6.5	1.6	2.9	2.9	0.5	0.5

[a] Numbers of different chains at peak-DP 85 as obtained by GPC.
[b] A-chains were detected as maltose after debranching; DP 3 is a sub-group of B1a(s)-chains; B1a(s) have DP 3–7; B1a(l), DP 8–17; B1b, DP 18–22; and B2, DP 23–52. B3-chains were not detected in clusters.

Table 7
Building block structure of clusters at peak-DP[a]

Samples	No. of blocks	IB-DP[b]	IB-CL[c]	Number of blocks of different groups[d]			
				2	3	4	5
Cr049-II	6.09	2.79	6.79	3.32	1.77	0.48	0.51
V69-II	6.00	2.75	6.75	3.19	1.79	0.44	0.59

[a] Numbers of different blocks at peak-DP 85 as obtained by GPC.
[b] Inter-block DP = (mol % linear blocks) × (DP of linear blocks)/(mol % of branched blocks).
[c] Inter-block CL, the approximate average length between building blocks inside the clusters,[14] = IB-DP + 4.
[d] (No. of blocks) × (relative molar distribution of groups of blocks from Table 4) of group 2 (DP 5–8), 3 (9–13), 4 (14–19), and 5 (⩾20).

suggest structural differences in both the intra- and inter-cluster levels, respectively, details of further investigations of which are necessary to be performed in order to be explained.

5. Conclusions

Two samples of amaranth amylopectins were investigated in this work. Both samples possessed clusters of comparatively homogenous size with average DP of 57 on a numerical basis. By mass, clusters of DP 82 predominated and were composed of ~13 chains distributed in ~6 tightly branched building blocks with an average ICL of 2.8–2.9 residues. The smallest possible blocks with only a single branch preponderated, however. Inside the clusters, the building blocks were interconnected through internal chain segments (IB-CL) of 6.8 residues at average. In contrast, the clusters were interconnected inside the amylopectins through far longer segments in the order of 11–14 residues (IC-CL).

Acknowledgments

This study was financially supported by the University of Hong Kong Committee on Research and Conference Grants.

References

1. Wang, Y. J.; White, P.; Pollak, L.; Jane, J. L. *Cereal Chem.* **1993**, *70*, 521–525.
2. Wang, L. Z.; White, P. J. *Cereal Chem.* **1994**, *71*, 263–268.
3. Nakamura, Y. *Plant Cell Physiol.* **2002**, *43*, 718–725.
4. Thompson, D. B. *Carbohydr. Polym.* **2000**, *43*, 223–239.
5. Hoover, R.; Sinnott, A. W.; Perera, C. *Starch/Stärke* **2000**, *52*, 456–463.
6. Radosavljevic, M.; Jane, J.; Johnson, L. A. *Cereal Chem.* **2000**, *75*, 212–216.
7. Qian, J. Y.; Kuhn, M. *Starch/Stärke* **1999**, *51*, 116–120.
8. Choi, H.; Kim, W.; Shin, M. *Starch/Stärke* **2004**, *56*, 469–477.
9. Kong, X. L.; Bao, J. S.; Corke, H. *Food Chem.* **2009**, *113*, 371–376.
10. Bello-Pérez, L. A.; Paredes-López, O.; Roger, P.; Colonna, P. *Food Chem.* **1996**, *56*, 171–176.
11. Bello-Pérez, L. A.; Paredes-López, O.; Roger, P.; Colonna, P. *Cereal Chem.* **1996**, *73*, 12–17.
12. Bello-Pérez, L. A.; Colonna, P.; Roger, P.; Paredes-López, O. *Cereal Chem.* **1998**, *75*, 395–402.
13. Bertoft, E. *Carbohydr. Polym.* **2007**, *68*, 433–446.
14. Bertoft, E. *Carbohydr. Polym.* **2007**, *70*, 123–136.
15. Kong, X. L.; Bertoft, E.; Bao, J. S.; Corke, H. *Int. J. Biol. Macromol.* **2008**, *43*, 377–382.
16. Bertoft, E.; Spoof, L. *Carbohydr. Res.* **1989**, *189*, 169–180.
17. Dubois, M.; Gilles, K. A.; Hamilton, J. K.; Rebers, P. A.; Smith, F. *Anal. Chem.* **1956**, *28*, 350–356.
18. Koch, K.; Andersson, R.; Åman, P. *J. Chromatogr., A* **1998**, *800*, 199–206.
19. Zhu, Q.; Bertoft, E. *Carbohydr. Res.* **1996**, *288*, 155–174.
20. Bertoft, E.; Zhu, Q.; Andtfolk, H.; Jungner, M. *Carbohydr. Polym.* **1999**, *38*, 349–359.
21. Gérard, C.; Planchot, V.; Colonna, P.; Bertoft, E. *Carbohydr. Res.* **2000**, *326*, 130–144.
22. Robyt, J.; French, D. *Arch. Biochem. Biophys.* **1963**, *100*, 451–467.
23. Bertoft, E.; Piyachomkwan, K.; Chatakanonda, P.; Sriroth, K. *Carbohydr. Polym.* **2008**, *74*, 527–543.
24. Hizukuri, S. *Carbohydr. Res.* **1986**, *147*, 342–347.
25. Bertoft, E. *Carbohydr. Polym.* **2004**, *57*, 211–224.
26. Ammeraal, R. N.; Delgado, G. A.; Tenbarge, F. L.; Friedman, R. B. *Carbohydr. Res.* **1991**, *215*, 179–192.
27. Bertoft, E. *Carbohydr. Res.* **1986**, *149*, 379–387.
28. Bertoft, E.; Koch, K. *Carbohydr. Polym.* **2000**, *41*, 121–132.
29. Pangborn, W.; Langs, D.; Pérez, S. *Int. J. Biol. Macromol.* **1985**, *7*, 363–369.
30. Imberty, A.; Pérez, S. *Carbohydr. Res.* **1988**, *181*, 41–55.
31. Umeki, K.; Yamamoto, T. *J. Biochem.* **1972**, *72*, 101–109.
32. O'Sullivan, A. C.; Pérez, S. *Biopolymers* **1999**, *50*, 381–390.
33. Angellier-Coussy, H.; Putaux, J.-L.; Molina-Boisseau, S.; Dufresne, A.; Bertoft, E.; Pérez, S. *Carbohydr. Res.* **2009**, *344*, 1558–1566.